

Graph Defense Diffusion Model

Xin He
Jilin University
Chang Chun, China
hexin20@mails.jlu.edu.cn

Wenqi Fan
The Hong Kong Polytechnic
University
Hong Kong, China
wenqifan03@gmail.com

Yili Wang
Jilin University
Chang Chun, China
wangyl21@mails.jlu.edu.cn

Chengyi Liu
The Hong Kong Polytechnic
University
Hong Kong, China
chengyi.liu@connect.polyu.hk

Rui Miao
Jilin University
Chang Chun, China
ruimiao20@mails.jlu.edu.cn

Xin Juan
Jilin University
Chang Chun, China
junxin22@mails.jlu.edu.cn

Xin Wang
Jilin University
Chang Chun, China
xinwangjlu@gmail.com

Abstract

Graph Neural Networks (GNNs) demonstrate significant potential in various applications but remain highly vulnerable to adversarial attacks, which can greatly degrade their performance. Existing graph purification methods attempt to address this issue by filtering attacked graphs; however, they struggle to effectively defend against multiple types of adversarial attacks simultaneously due to their limited flexibility, and they lack comprehensive modeling of graph data due to their heavy reliance on heuristic prior knowledge. To overcome these challenges, we propose a more versatile approach for defending against adversarial attacks on graphs. In this work, we introduce the **Graph Defense Diffusion Model (GDDM)**, a flexible purification method that leverages the denoising and modeling capabilities of diffusion models. The iterative nature of diffusion models aligns well with the stepwise process of adversarial attacks, making them particularly suitable for defense. By iteratively adding and removing noise, GDDM effectively purifies attacked graphs, restoring their original structure and features. Our GDDM consists of two key components: (1) Graph Structure-Driven Refiner, which preserves the basic fidelity of the graph during the denoising process, and ensures that the generated graph remains consistent with the original scope; and (2) Node Feature-Constrained Regularizer, which removes residual impurities from the denoised graph, further enhances the purification effect. Additionally, we design tailored denoising strategies to handle different types of adversarial attacks, improving the model’s adaptability to various attack scenarios. Extensive experiments conducted on three real-world datasets demonstrate that GDDM outperforms state-of-the-art methods in defending against a wide range of adversarial attacks, showcasing its robustness and effectiveness.

CCS Concepts

• Information systems → Data mining.

Keywords

Graph Neural Networks, Adversarial Attack, Diffusion Model

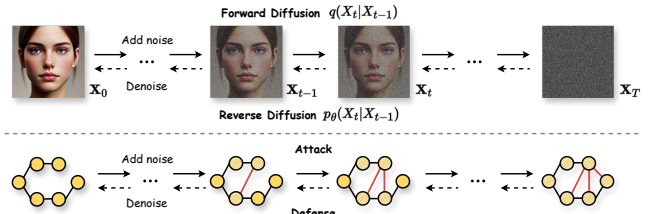


Figure 1: The connection between graph adversarial attack, defense and diffusion model.

1 INTRODUCTION

Graph data, characterized by its ability to capture complex relationships within real-world systems, has become increasingly prevalent across diverse domains, such as recommendation systems [8, 14], biological networks [21, 26], and social sciences [5, 9]. The complexity and richness of graph structures provide a unique opportunity to extract meaningful insights from interconnected entities. However, the very characteristics that make graph data valuable also make it particularly vulnerable to adversarial attacks. Subtle modifications to graph structures or node features can drastically alter model outcomes, posing significant challenges in maintaining the reliability of graph-based learning systems.

Building on the potential of graph data, GNNs have emerged as a particularly effective approach to representation learning, leveraging message-passing mechanisms to aggregate both structural and feature information. This capability has enabled GNNs to achieve considerable success in downstream tasks such as node classification, link prediction, and graph classification [12, 23, 35], but it also makes them vulnerable to adversarial attacks that exploit their dependence on interconnected features and structures [18, 20, 29]. These attacks involve subtle, often imperceptible modifications to graph structures or node features, leading to significant degradation in model performance. Such attacks can be categorized into targeted attacks, which focus on misclassifying specific nodes, and

untargeted attacks, which aim to disrupt the overall graph integrity. The ability of these attacks to compromise model reliability poses serious challenges, especially in critical domains such as fraud detection, healthcare, and cybersecurity, where the consequences of incorrect predictions can be severe.

To counter these threats, effective defense mechanisms are needed to enhance the robustness of GNNs. Graph purification methods have shown promise by reconstructing attacked graphs without modifying the underlying GNN model. These methods are efficient and avoid the complexity of adversarial training routines [19]. However, current purification approaches often lack adaptability to diverse attack strategies [24], and many depend heavily on heuristic-based prior knowledge rather than comprehensive modeling of the graph distribution [37]. This motivates us to pose the following research question: **how can we develop a more versatile and effective framework that flexibly adapts to different adversarial scenarios and accurately reconstructs clean graphs?**

Diffusion models represent a promising strategy for addressing challenges associated with adversarial attacks on graphs, drawing on their demonstrated success in image generation and denoising [10, 30, 31]. As shown in Fig. 1, the forward diffusion process perturbs the data with random noise, stimulating the adversarial attacks to disrupt the graphs. Correspondingly, the reverse process reconstructs samples from noise, whose objective aligns well with the defense methods. However, no prior work has employed graph diffusion models to defend against graph adversarial attacks, primarily due to two key challenges: ① **Graph fidelity**: purifying high-fidelity graphs directly is difficult due to the complexity of graph topology and the inherent minor noise in the original graph [18, 33]. ② **Localized denoising**: current diffusion models perform global denoising, making it hard to focus on specific nodes or edges affected by targeted attacks.

In this paper, we propose the **Graph Defense Diffusion Model (GDDM)** to enhance the inference phase of vanilla diffusion models, aiming to address the two aforementioned challenges. Supervised by different levels of graph labels (e.g., adjacency matrix and node feature), GDDM implements targeted interventions on the current formation state to maximize its fidelity to the ground truth: During the denoising process, **Graph Structure-Driven Refiner (GSDR)** filters out the incorrect edges step-by-step while preserving plausible connections, serving as the guarantee of the basic fidelity. At the end of the denoising process, **Node Feature-Constrained Regularizer (NFCR)** utilizes node features to remove residual impurities unintentionally introduced during denoising, enabling precise corrections without compromising the overall graph structure. The coupling of these two components provides reliable quality control throughout the entire denoising process, collaboratively ensuring graph fidelity (Challenge 1). We also design **Tailored Attack-specific Denoising Strategies (TADS)** to retain non-target edges as the foundation of the denoising process, achieving localized denoising (Challenge 2).

In the **training phase**, we simplify the GDDM by focusing on the critical elements necessary for defending against adversarial attacks, which reduces the model’s complexity while retaining its effectiveness. Instead of learning the entire process of reconstructing the graph, we take advantage of sampling techniques to calculate intermediate steps.

The contributions of this work are summarized as follows:

- **Novel Graph Defense Framework:** We propose the Graph Defense Diffusion Model (GDDM), which introduces a diffusion model-based approach to effectively defend against graph adversarial attacks, addressing both graph fidelity and localized denoising challenges.
- **Graph Fidelity Enhancement Components:** We introduce two key components: the Graph Structure-Driven Refiner (GSDR) and the Node Feature-Constrained Regularizer (NFCR). Their integration ensures high-fidelity denoised graphs through different levels of graph labels.
- **Tailored Denoising Strategies:** We design Tailored Attack-Specific Denoising Strategies (TADS) to remove the edges related to the target nodes from the initial adjacency matrix in targeted attack scenarios, achieving localized denoising.
- **Strong Experimental Results:** Our extensive experiments demonstrate that GDDM provides superior performance in defending against different types of adversarial attacks, outperforming current state-of-the-art methods.

2 Related Work

2.1 Adversarial Attack on Graphs

Graph Neural Networks (GNNs) have been highly successful in graph data mining, but they are vulnerable to adversarial perturbations due to their dependency on the graph structure and message-passing mechanism [2, 11, 28]. One type of adversarial attack targets specific nodes in the graph, known as targeted attacks. IG-FGSM [37] is an integrated gradients-based method that outperforms existing iterative and gradient-based techniques. Net-tack [43] uses a greedy approach to perturb targeted nodes without altering node degree or feature co-occurrence. Another type of attack targets the entire graph, known as non-targeted attacks. Met-tack [44] is a classic method using meta-learning for global graph attacks, but it is inefficient due to its focus on low-confidence nodes. GraD [28] improves the attack by focusing on medium-confidence nodes, enhancing efficiency.

2.2 Graph Defense Methods

To counter adversarial attacks, various defense strategies have been proposed [17, 40–42]. One type of effective defense method is graph purification. Jaccard [37] defends against adversarial attacks by pruning edges based on the feature similarity between the two connected nodes. SVD [7] defends against adversarial attacks by removing the high-rank perturbations introduced by the attack methods. Guard [24] preemptively removes all potential noisy edges by node degree information to protect target nodes. Another type of method is GNN-improved, which improves the robustness of GNNs by enhancing the GNN models themselves. ProGNN [19] and STABLE [25] mitigate the negative effects of adversarial attacks on GNNs by graph structure learning to filter out the noisy edges. Elastic [27] allows the model to tolerate more noisy edges in the graph, making it more robust against adversarial attacks on graph data. Although existing defense methods achieve significant success, graph purification methods are unable to defend against multiple types of adversarial attacks.

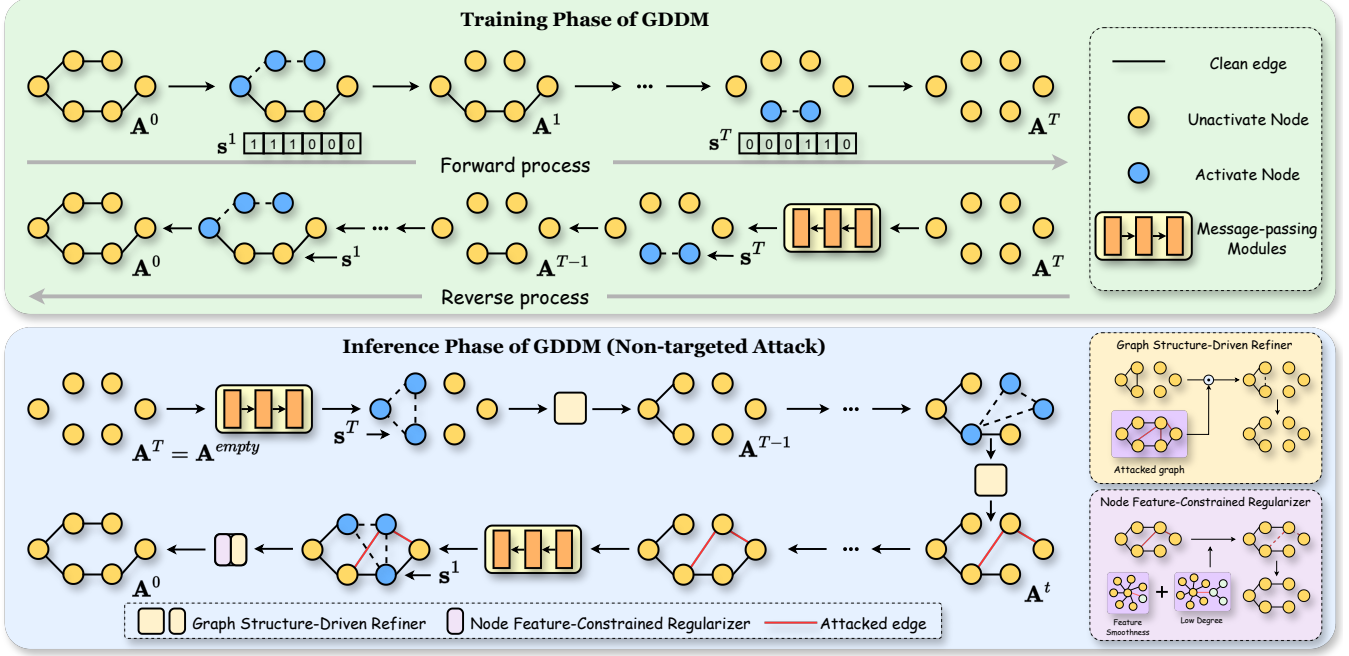


Figure 2: The Framework of GDDM.

2.3 Diffusion Models for Graph Data

Diffusion models [1, 3, 6, 39] have shown success in generating molecular and material graphs. GDSS [21] models the joint distribution of nodes and edges using stochastic differential equations to generate desired molecular graphs. DiGress [36] models a discrete diffusion process, performing graph denoising by changing types of edges at each recovery step. EDGE [4] models the change of each edge in the diffusion process as a Bernoulli distribution and introduces a guidance mechanism during recovery, significantly improving training efficiency and enabling the possibility of training diffusion models on large graphs. Although diffusion models excel at denoising, they have yet to be applied to adversarial graph defense. We observe a natural alignment between their processes and the dynamics of adversarial attacks and defenses, proposing a graph diffusion model with different denoising strategies guided by two fidelity enhancement components to defend against different types of graph adversarial attacks.

3 PRELIMINARY

3.1 Problem Statement

Let $\mathcal{G} = (\mathcal{V}, \mathcal{E}, \mathbf{A}, \mathbf{X})$ be an undirected graph, where $\mathcal{V} = \{v_1, \dots, v_N\}$ is the set of N nodes and \mathcal{E} is the set of edges. The adjacency matrix $\mathbf{A} \in \mathbb{R}^{N \times N}$ represents the connectivity between nodes, where $A_{ij} = 1$ if there is an edge between node v_i and node v_j , and $A_{ij} = 0$ otherwise. The node feature matrix $\mathbf{X} \in \mathbb{R}^{N \times d}$ contains a d -dimensional feature vector for each node. Thus, a graph can also be compactly represented as $\mathcal{G} = (\mathbf{A}, \mathbf{X})$, where \mathbf{A} encapsulates structural information and \mathbf{X} represents node features. In the context of node classification tasks, adversarial attacks introduce perturbations primarily into the adjacency matrix \mathbf{A} and sometimes

into the feature matrix \mathbf{X} , which leads to a degradation in the performance of GNN classifiers. Let $\mathcal{G}' = (\mathbf{A}', \mathbf{X}')$ be the perturbed graph, where \mathbf{A}' and \mathbf{X}' denote the adversarially perturbed adjacency and feature matrices, respectively. In this work, we specifically consider the scenario where the feature matrix \mathbf{X} remains unchanged, i.e., $\mathcal{G}' = (\mathbf{A}', \mathbf{X})$, and only the adjacency matrix \mathbf{A} is compromised by adversarial edges. The goal is to employ a graph diffusion model to remove as many adversarial edges as possible from the perturbed graph \mathcal{G}' , thus improving the accuracy of downstream GNN classifiers in the node classification task.

3.2 Discrete Graph Diffusion and Recovery

The Discrete Graph Diffusion Model represents the noise injection process using a Binomial distribution [34], based on the assumption that each edge modification during noise injection is independent. In this setup, the adjacency matrix $\mathbf{A} \in \mathbb{R}^{N \times N}$ of the target graph \mathcal{G} is a binary matrix with zeros on the diagonal. Let \mathbf{A}^0 denote the original adjacency matrix of the target graph. We then define the diffusion process as $q(\mathbf{A}^t | \mathbf{A}^{t-1})$ with t denoting the timestep. In the forward diffusion process, a Bernoulli distribution $\mathcal{B}(x; \mu)$ over x with probability μ is used to represent the probability of each edge being resampled at the current timestep t :

$$\begin{aligned} q(\mathbf{A}^t | \mathbf{A}^{t-1}) &= \prod_{i,j} \mathcal{B}(A_{i,j}^t; (1 - \beta_t)A_{i,j}^{t-1} + \beta_t p) \\ &= \mathcal{B}(\mathbf{A}^t; (1 - \beta_t)\mathbf{A}^{t-1} + \beta_t p), \end{aligned} \quad (1)$$

where β_t is the diffusion rate controlling the probability of resampling the element $A_{i,j}^t$ from the Bernoulli distribution with probability p , rather than keeping the original $A_{i,j}^{t-1}$. Therefore, this specific diffusion process allows direct sampling of \mathbf{A}^t from \mathbf{A}^0 :

$$q(\mathbf{A}^t | \mathbf{A}^0) = \mathcal{B}(\mathbf{A}^t; \bar{\alpha}_t \mathbf{A}^0 + (1 - \bar{\alpha}_t)p), \quad (2)$$

where $\alpha_t = 1 - \beta_t$ and $\bar{\alpha}_t = \prod_{i=1}^t \alpha_i$. As t approaches infinity, $\bar{\alpha}_t$ converges to 0, meaning that the final adjacency matrix A^T becomes fully independent of the original A^0 . The value of p controls the probability of forming edges in A^T , where higher values of p imply a denser graph.

During the denoising process, the goal is to reverse the diffusion process by reconstructing A^{t-1} from A^t , using a trained model to approximate the posterior distribution:

$$q(A^{t-1}|A^t, A^0) = \frac{q(A^t|A^{t-1})q(A^{t-1}|A^0)}{q(A^t|A^0)}. \quad (3)$$

Since all terms are known, the model can directly compute Eq.3 for recovering the original graph structure during training.

4 Graph Defense Diffusion Model

The architecture of the Graph Defense Diffusion Model (GDDM) is illustrated in Fig. 2, comprising two key components: the training phase and the inference phase. In the **training phase**, GDDM is trained on clean graph data leveraging a simplified discrete graph diffusion model. We reduce the model's complexity by employing sampling techniques for intermediate step calculations, enhancing training efficiency while maintaining the ability to reconstruct clean graph structures. During the **inference phase**, we introduce two components: the graph structure-driven refiner and the node feature-constrained regularizer. These components ensure high-fidelity denoised graph while enhancing GDDM's ability to defend against adversarial attacks. Additionally, we incorporate tailored attack-specific denoising strategies to effectively address different types of adversarial attacks, allowing GDDM to flexibly adapt its defense mechanism based on the nature of the attack. In the following sections, we will provide detailed explanations of these components.

4.1 The Training Phase

4.1.1 Forward and Recovery. Given the complexity and high dimensionality of graph data, direct training on all node and edge relationships can be computationally intensive and inefficient. To address this challenge while preserving the model's ability to accurately reconstruct graph structures, we simplify the model by introducing a state vector s^t [4], which tracks the nodes with degree changes at each timestep of the discrete graph diffusion process. This simplification reduces computational overhead while maintaining the model's ability to restructure graphs effectively. Specifically, the state vector s^t indicates whether the degree of node i changes between timestep $t - 1$ and t . If the degree changes, s_i^t is set to 1, otherwise 0. The **forward diffusion process** of GDDM can be formalized as:

$$q(A^t, s^t|A^{t-1}) = q(A^t|A^{t-1}) = \mathcal{B}(A^t; (1 - \beta_t)A^{t-1} + \beta_t p). \quad (4)$$

where β_t controls the probability of resampling edges. Notably, the introduction of s^t does not modify the core diffusion process but provides a mechanism to track which nodes' degrees are altered. Furthermore, setting $p = 0$ transforms the forward diffusion into an edge removal process. During the **denoising process**, we train a message-passing neural network $p_\theta(A^{t-1}|A^t)$ to approximate the

posterior of the forward process:

$$q(A^{t-1}|A^t, s^t, A^0) = \frac{q(A^t|A^{t-1})q(s^t|A^t, A^{t-1})q(A^{t-1}|A^0)}{q(A^t|A^0)q(s^t|A^t, A^0)}. \quad (5)$$

Further derivation details are provided in Appendix A.1. In each recovery step, the network computes the state vector s^t , which identifies the nodes for which edges should be generated. The recovery process is decomposed as follows:

$$p_\theta(A^{t-1}|A^t) = p_\theta(A^{t-1}|s^t, A^t)p_\theta(s^t|A^t). \quad (6)$$

Although this decomposition introduces new optimization objectives, previous work [38] has shown a strong correlation between the state vector s^t and the degree vectors d^0 and d^t . The state vector can be predicted as:

$$q(s^t|d^t, d^0) = \prod_{i=1}^N q(s_i^t|d_i^t, d_i^0), \quad (7)$$

$$q(s_i^t|d_i^t, d_i^0) = \mathcal{B}(s_i^t; 1 - (1 - \frac{\beta_t \bar{\alpha}_{t-1}}{1 - \bar{\alpha}_{t-1}})^{d_i^0 - d_i^t}),$$

where N represents the total number of nodes in the graph, $\alpha_t = 1 - \beta_t$ and $\bar{\alpha}_t = \prod_{i=1}^t \alpha_i$. During the training phase, the optimization is focused only on $p_\theta(A^{t-1}|s^t, A^t)$. The state vector s^t is directly sampled from the degree vectors d^0 and d^t , which simplifies the training phase by eliminating the need for additional optimization of $p_\theta(s^t|A^t)$, thus improving computational efficiency without compromising model performance.

4.1.2 Optimization Objective. Building on the recovery process discussed earlier, we now define the optimization objective for GDDM. To optimize the parameters θ , we maximize the variational lower bound (VLB) [15, 32] of $\log p(A^0)$, ensuring that the model learns to accurately reconstruct the original graph from its perturbed version. The optimization objective is defined as follows:

$$\mathcal{L} = \mathbb{E}_q \left[\log \frac{p(A^T)}{q(A^T|A^0)} + \log p_\theta(A^0|A^1, s^1) + \sum_{t=2}^T \log \frac{p_\theta(A^{t-1}|A^t, s^t)}{q(A^{t-1}|A^t, A^0, s^t)} \right]. \quad (8)$$

The first term does not involve learnable parameters, while Monte Carlo estimation [13] is used to optimize the second and third terms. This process enables GDDM to iteratively reconstruct the graph from an empty state, capturing its structure and improving denoising performance. The overall training phase of GDDM is presented in Appendix A.3.

4.1.3 Model Structure. To better understand how GDDM functions, we now provide an overview of its internal structure. GDDM consists of two main components: information propagation and edge prediction, which work together to reconstruct the graph from an empty structure iteratively.

In the information propagation process, node degree representations are used to capture features. The initial representation of each node is constructed by concatenating the node's initial d^0 with its current degree d^t , along with the timestep t and global contextual features c . This can be formulated as:

$$Z_i^0 = \text{concat}(\text{emb}_d(d_i^t) || \text{emb}_d(d_i^0)), \quad (9)$$

$$\mathbf{t}_{emb} = \text{emb}_t(t), \mathbf{c}^0 = \text{mean}(\mathbf{Z}^0), \quad (10)$$

where $\text{concat}(\cdot)$ represents the concatenation operation, $\text{emb}_d(\cdot)$ and $\text{emb}_t(\cdot)$ represent the degree and time encoding functions, and \mathbf{c}^0 captures the initial global context. Then, these initial node representations are updated iteratively as follows:

$$\mathbf{Z}^l, \mathbf{c}^l, \mathbf{H}^l = \text{MPM}(\mathbf{Z}^{l-1}, \mathbf{t}_{emb}, \mathbf{c}^{l-1}, \mathbf{H}^{l-1}), \quad (11)$$

where \mathbf{H} refers to the node hidden features at each layer l . The message-passing mechanism (MPM) propagates information across the graph to refine the node representations iteratively. The detail of the information propagation process is in Appendix A.2.

For edge prediction, after L iterations of updates, a multi-layer perceptron (MLP) is used to predict whether an edge should be generated between nodes i and j . The prediction is based on the final representations \mathbf{Z}_i^L and \mathbf{Z}_j^L of the nodes:

$$b_{i,j}^{t-1} = \text{MLP}(\mathbf{Z}_i^L + \mathbf{Z}_j^L), \text{ where } (i, j) \in \{(i, j) | s_{i,j}^t = 1\}, \quad (12)$$

where $b_{i,j}^{t-1}$ is the predicted two-dimensional Bernoulli parameter for generating an edge between node i and node j . Then, whether an edge is generated between nodes i and j is determined by a sampling process based on $b_{i,j}^{t-1}$ and a Gumbel noise [16] g with the same dimensionality as $b_{i,j}^{t-1}$, which can be defined as follows:

$$\mathbf{A}_{i,j}^{t-1} = \arg \max(b_{i,j}^{t-1} + g). \quad (13)$$

4.2 The Inference Phase

Following the completion of the training phase, GDDM applies the learned diffusion dynamics to reconstruct the clean graph from the attacked one. During inference, the process iteratively restores the graph by sampling the state vector \mathbf{s}^t and adjacency matrix \mathbf{A}^{t-1} at each timestep, as defined by:

$$\mathbf{s}^t \sim q(\mathbf{s}^t | \mathbf{d}^t, \mathbf{d}^0), \quad (14)$$

$$\mathbf{A}^{t-1} \sim p_\theta(\mathbf{A}^{t-1} | \mathbf{s}^t, \mathbf{A}^t), \quad (15)$$

where \mathbf{d}^0 is the degree vector of the attacked graph, \mathbf{d}^t is the degree vector at timestep t , and p_θ represents the learnable network.

Following the sampling steps in inference, the next crucial task is to ensure that the generated graph maintains a high-fidelity with the attacked graph. This is essential to ensure that while adversarial noise is mitigated, the core structure of the original graph is preserved. To achieve this, GDDM integrates two core components: Graph Structure-Driven Refiner (GSDR) and Node Feature-Constrained Regularizer (NFCR). Additionally, tailored denoising strategies are employed to handle various types of adversarial attacks, allowing GDDM to effectively target both global and localized attacks.

4.2.1 Graph Structure-Driven Refiner (GSDR). GSDR is designed to tackle the challenge of generating high-fidelity graphs during the denoising process. Due to the complexity of graph topology and the inherent noise in the original graph, directly generating a high-fidelity graph is difficult. GSDR addresses this by incrementally refining the graph structure at each timestep. At each step of the generation process, GSDR filters out incorrect edges, ensuring that

only edges consistent with the attacked graph are retained. This process is formalized as:

$$\mathbf{A}^t = \mathbf{A}' \odot \mathbf{A}^t, \quad (16)$$

where \mathbf{A}' represents the adjacency matrix of the attacked graph, \mathbf{A}^t represents the adjacency matrix of the corresponding graph at timestep t during the generation process. The element-wise multiplication \odot preserves the intersection between \mathbf{A}' and \mathbf{A}^t . By filtering edges step-by-step, GSDR preserves plausible connections while removing adversarial noise, ensuring the generated graph remains structurally consistent with the attacked graph.

4.2.2 Node Feature-Constrained Regularizer (NFCR). While GSDR effectively removes the most noisy edges, residual noise in node features can still affect the overall graph quality. NFCR refines the generated graph by incorporating node feature and degree information, which addresses residual noise that remains after structural pruning. NFCR ensures that both node features and the underlying graph structure are preserved, enhancing the fidelity of the generated graph. NFCR operates in two stages: feature smoothness guiding and node degree guiding.

Feature smoothness guiding. As the generated graph reaches a certain size, it becomes necessary to evaluate whether the generated edges connect nodes that should logically be connected. This is achieved by assessing the feature smoothness between pairs of nodes connected by the generated edges. The feature smoothness is calculated as follows:

$$\text{FS}(i, j) = \|\mathbf{X}_i - \mathbf{X}_j\|_2^2, \quad (17)$$

where \mathbf{X} is the feature matrix of the original graph. Each row vector \mathbf{X}_i or \mathbf{X}_j in the feature matrix \mathbf{X} represents the one-hot vector of a node, $\|\cdot\|_2^2$ represents the square of the second-order norm of the vector. $\text{FS}(i, j)$ represents the feature smoothness between the two nodes, with higher values indicating lower feature similarity and a reduced likelihood of an edge existing between them. After calculating the feature smoothness for all edges in the generated graph, the top- k edges with the highest smoothness values (i.e., lowest feature similarity) are removed. This step ensures that only edges connecting nodes with similar features are retained, improving the quality of the generated graph.

Node degree guiding. In addition to feature smoothness, the node degrees of the connected nodes also play a crucial role in determining whether an edge should be retained. Previous studies, such

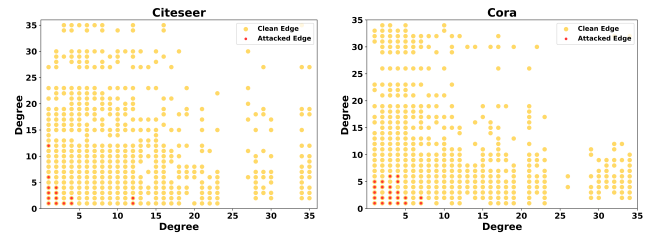


Figure 3: Edges distribution of Attacked Graph based on degree (Cora and Citeseer). A point may represent multiple edges, and attacked edges (red points) will always cover clean edges (yellow points).

Algorithm 1 The Inference Phase of GDDM

Input: The initial empty graph adjacency matrix A^{empty} for non-targeted attack method, the initial graph adjacency matrix A^{tar} for targeted attack method, the degree vectors \mathbf{d}_0 of attacked graph, the attacked graph adjacency matrix A' , the diffusion schedule β , the model parameter θ , the desired graph size ratio μ .

Output: The denoised graph adjacency matrix A^0 .

- 1: $A^T = A^{empty}$ for non-targeted attack or $A^T = A^{tar}$ for targeted attack.
- 2: **while** $t = T, \dots, 1$ and the scale of A^t reach the desired graph size ratio μ **do**
- 3: Obtain A^{t-1} via Eq. 14 and Eq. 15.
- 4: Use the adjacency matrix of the attacked graph A' to filter A^{t-1} via Eq. 16.
- 5: **if** $t = 1$ **then**
- 6: Set $A^T = A^0$.
- 7: Set $t = T/2$.
- 8: **end if**
- 9: **end while**
- 10: Further filter A^0 based on feature smoothness and node degrees via Eq. 17 and Eq. 18.
- 11: Obtain the final denoised graph adjacency matrix A^0 .

as GraD [28], reveal that graph attack methods tend to target low-degree nodes by introducing noisy edges that connect these vulnerable nodes. To explore this, we visualize the distribution of edges in the attacked graph, as shown in Fig. 3. In the visualization, the yellow points represent the edges that originally existed in the graph, while the red points indicate the noisy edges introduced by the attack methods; the horizontal and vertical axes correspond to the degrees of the two nodes connected by each edge in the original graph. As shown in the figure, attack methods frequently add edges that involve at least one low-degree node. This pattern indicates that low-degree nodes are more susceptible to being targeted by these attacks.

To address this vulnerability, the node degree information is integrated into the edge filtering process. Specifically, if an edge exhibits high feature smoothness (indicating a low likelihood of existence) and involves low-degree nodes, it is likely to be a noisy edge introduced by the attack. The probability of an edge being targeted by an attack is defined as:

$$P_{\text{attack}}(i, j) = \begin{cases} 1 & \text{if } d(i) < \lambda \text{ or } d(j) < \lambda \\ 0 & \text{else} \end{cases}, \quad (18)$$

where $d(\cdot)$ represents the degree of the target node in the attacked graph. λ represents the threshold, which varies depending on the dataset. After an edge is flagged based on node degrees, it undergoes further evaluation using feature smoothness. If $P_{\text{attack}}(i, j) = 1$ and the edge rank within the top- k in terms of feature smoothness, the edge is removed from the generated graph. Otherwise, the edge is retained.

By combining feature smoothness and node degree filtering, NFCR effectively removes noisy edges, especially those from low-degree nodes targeted by adversarial attacks. Together with GSDR, which ensures structural consistency by pruning incorrect edges,

these components work to maintain the fidelity of the generated graph. While GSDR focuses on preserving the correct structure, NFCR refines node-level details, ensuring a clean and accurate graph, addressing **Challenge 1: Graph Fidelity**.

4.2.3 Tailored Attack-Specific Denoising Strategies. While GSDR and NFCR address the global fidelity of the graph, targeted attacks require more localized denoising strategies. To address **Challenge 2: localized denoising**, GDDM adopts tailored strategies for different types of adversarial attacks. For **non-targeted attacks**, the adjacency matrix A^{empty} of an empty graph is used as the starting point, allowing GDDM to reconstruct the entire graph from scratch. This global denoising process ensures that all edges are regenerated, as shown in Fig. 2. For **targeted attacks**, where specific nodes are compromised, a more focused strategy is necessary. GDDM starts by removing all edges connected to the target nodes, constructing an initial adjacency matrix A^{tar} , defined as:

$$A^{tar} = A' - A'', \quad (19)$$

where A' represents the adjacency matrix of the attacked graph, A'' represents the adjacency matrix containing only the edges connected to the target nodes. This allows GDDM to perform localized denoising, focusing on the areas most affected by the attack, as shown in Appendix A.4. The overall inference phase of GDDM is presented in Algorithm 1.

5 Experiment

In this section, we present an empirical evaluation of GDDM's defense effectiveness and robustness against different adversarial attacks. Specifically, we seek to address the following key research questions (RQs):

- **(RQ1)** Does GDDM outperform state-of-the-art defense models across various types of adversarial attacks?
- **(RQ2)** Does our designed denoising strategy enhance GDDM's ability to protect specific nodes under targeted attack?
- **(RQ3)** Do the additional components improve the model's defense effectiveness against various attack methods?
- **(RQ4)** Does GDDM flexibly integrate with different downstream GNNs and remain effective?
- **(RQ5)** How does the performance of GDDM vary with different hyper-parameters?

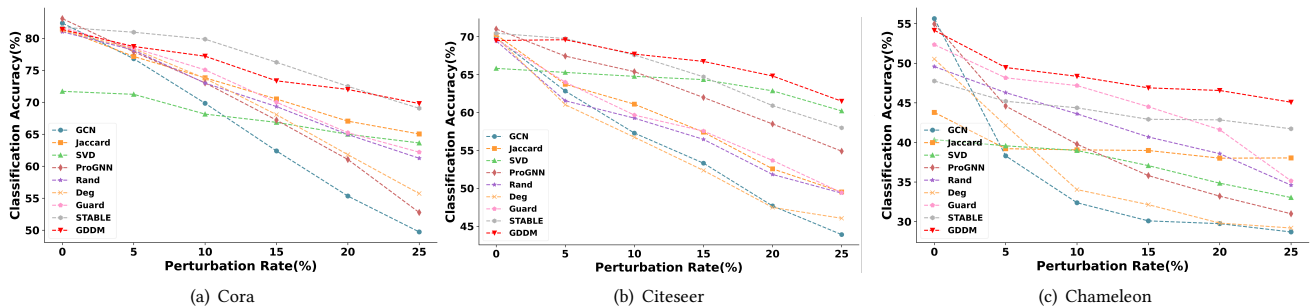
5.1 Experimental Settings

5.1.1 Dataset. We conduct our experiments on three benchmark datasets under non-targeted attack (GraD [28]) and targeted attack (Nettack [43]), consisting of two citation graphs, Cora and Citeseer, and a page-page heterogeneous graph, Chameleon. When processing the Chameleon dataset, we treated it as a homogeneous dataset by considering all edges as a single category. The statistics for these datasets are provided in Appendix B.1.

5.1.2 Baselines. We compare GDDM with representative and state-of-the-art defense methods to evaluate its robustness. These baseline models include classical GNNs method GCN [22], improved GCNs methods ProGNN [19], STABLE [25], and graph purification methods Jaccard [37], SVD [7], Rand [24], Deg [24], Guard [24].

Table 1: Node classification performance (Accuracy±Std) under targeted attack (Nettack).

Datasets	Ptb Num	GCN	Jaccard	SVD	ProGNN	Rand	Deg	Guard	STABLE	GDDM
Cora	0	81.46±1.04	78.88±0.67	77.64±2.48	83.26±0.79	79.66±1.17	81.91±0.93	81.35±1.15	81.01±0.98	<u>82.02±1.00</u>
	1	75.51±1.31	74.27±0.93	78.09±1.61	77.53±1.59	74.16±1.88	77.19±1.82	<u>78.88±1.57</u>	78.31±1.50	81.34±1.43
	2	71.01±1.57	70.11±1.25	76.97±1.15	74.16±1.00	68.31±1.21	70.67±2.33	75.84±1.35	<u>76.52±0.98</u>	81.46±1.03
	3	67.87±1.76	68.09±1.03	71.46±2.02	67.53±0.79	66.63±1.43	65.84±1.60	69.21±1.35	<u>73.60±0.95</u>	80.78±0.93
	4	63.93±1.98	64.94±1.73	70.45±3.30	65.06±2.38	61.57±2.00	62.25±1.83	65.96±0.88	<u>72.69±0.93</u>	79.77±1.01
	5	57.64±1.88	63.15±1.73	64.04±3.41	57.19±2.63	56.29±1.37	57.08±2.50	61.91±1.46	<u>68.65±1.35</u>	78.65±1.74
	Mean	69.72	69.91	73.11	70.79	67.77	69.16	72.19	<u>75.13</u>	80.56
Citeseer	0	83.12±1.12	82.71±0.83	78.02±1.35	83.23±0.96	83.12±1.12	<u>83.85±0.96</u>	83.54±0.78	85.00±1.91	83.03±1.05
	1	76.25±1.38	77.50±2.60	78.12±0.81	81.25±1.80	74.79±1.67	77.19±3.31	79.69±1.82	84.47±1.73	<u>82.50±1.21</u>
	2	60.10±4.52	65.62±2.13	69.90±2.35	69.68±5.86	64.58±2.64	57.19±3.17	<u>74.17±0.78</u>	70.83±4.42	81.25±1.47
	3	54.48±1.92	64.79±3.01	70.00±1.21	58.64±2.47	61.77±3.67	53.96±3.63	<u>73.65±1.68</u>	64.69±3.42	81.87±1.06
	4	48.44±2.43	58.12±1.67	62.08±3.13	53.23±1.35	57.19±1.89	46.46±1.25	<u>71.77±2.16</u>	61.04±2.21	82.60±1.61
	5	43.33±2.95	52.50±1.99	57.40±4.26	47.50±4.57	46.15±4.89	42.71±1.47	<u>63.44±3.00</u>	56.04±4.57	81.46±1.02
	Mean	60.95	66.87	69.25	65.59	64.60	60.23	<u>74.27</u>	70.35	82.01
Chameleon	0	59.20±0.42	45.61±1.96	50.57±1.05	58.64±1.01	54.34±0.58	58.53±1.11	<u>59.00±0.74</u>	51.11±1.68	58.01±0.86
	1	54.58±0.70	43.74±1.08	49.84±0.85	53.93±0.82	48.77±1.02	56.10±0.48	<u>56.56±0.60</u>	48.93±0.21	58.45±0.90
	2	50.62±0.87	41.44±1.20	49.35±0.82	48.67±1.41	42.30±1.20	53.15±1.06	<u>54.50±0.87</u>	47.53±2.17	56.60±0.69
	3	47.20±0.67	40.07±1.20	48.23±0.79	43.64±1.53	38.75±1.11	47.58±1.44	<u>51.60±1.01</u>	47.33±0.88	55.48±0.97
	4	42.84±1.48	39.96±1.19	47.40±0.78	40.23±1.34	36.44±1.10	44.51±1.25	<u>48.66±1.76</u>	46.96±1.49	54.83±0.48
	5	40.63±2.19	37.99±1.27	45.74±0.94	37.06±1.92	35.67±1.41	41.45±1.73	<u>45.88±2.71</u>	46.52±2.49	54.76±0.81
	Mean	49.18	41.47	48.52	47.03	42.71	50.22	<u>52.7</u>	48.06	56.34

**Figure 4: Node classification performance (Accuracy±Std) under non-targeted attack (Grad).**

For the experiments, we implement a non-targeted structural adversarial attack, **Grad** [28], and a targeted structural adversarial attack, **Nettack** [43]. Detailed descriptions of these defense and attack methods are provided in Appendix B.2.

5.1.3 Implementation Details. For each graph, we randomly split the nodes into 10% for training, 10% for validation, and 80% for testing. We then generate attacks on each graph based on the perturbation number/rate, and we ensure that all hyper-parameters in the attack methods align with the original authors' implementations. During the model training phase, we primarily adjust the diffusion steps, with a range of {64, 128, 256, 512}. During the model inference phase, we primarily adjust the expected size of the generated graph, ranging from 70% to 95%. Performance is reported as the average accuracy with standard deviation, based on 10 runs on clean, perturbed or denoised graphs. We closely follow the default setting of the baselines for a fair comparison.

5.2 Robustness Evaluation (RQ1)

5.2.1 Performance Against Targeted Attack. Table 1 presents the performance on three datasets against targeted attack (Nettack [43]). We set the perturbation number for targeted node between 1 and 5 with the step of 1. Following prior work [19], we selected nodes with degrees larger than 10 in the test set as target nodes for the targeted attacks. The top two results are highlighted in bold and underline. From this main experiment, we make the following observations:

- The performance of all the methods declines as the perturbation number increases, demonstrating the effectiveness of the attack method. In most cases, GCN shows the largest performance drop, proving that its ability to defend against adversarial attacks is particularly weak.
- Jaccard and SVD are feature-based edge pruning methods. Compared to other baseline methods, Jaccard and SVD exhibit relatively lower sensitivity to perturbations. However, they are insufficient to completely remove adversarial edges

Table 2: Results of denoising strategies for a targeted attack.

Datasets	Ptb Num	GDDM w/o TADS	GDDM
Cora	0	80.80±1.57	81.34±0.75
	1	77.41±0.85	81.34±1.43
	2	72.58±1.35	81.46±1.03
	3	70.79±1.23	80.78±0.93
	4	66.06±1.87	79.77±1.01
	5	62.13±2.71	78.65±1.74
	Mean	71.63	80.56
Citeseer	0	82.02±1.48	82.40±1.27
	1	81.25±1.55	82.50±1.21
	2	78.75±1.87	81.25±1.47
	3	78.02±1.51	81.87±1.06
	4	76.88±2.02	82.60±1.61
	5	79.06±1.58	81.46±1.02
	Mean	79.33	82.01
Chameleon	0	57.88±0.52	58.01±0.86
	1	57.51±0.93	58.45±0.90
	2	55.69±0.98	56.60±0.69
	3	55.31±1.16	55.48±0.97
	4	52.26±0.80	54.83±0.48
	5	53.93±1.25	54.76±0.81
	Mean	55.43	56.36

and may even mistakenly delete clean edges, leading to performance degradation on clean graphs.

- The improved GCNs methods ProGNN and STABLE achieve outstanding performance at low perturbation numbers, but their performance drops sharply as the perturbation number increases. This may be due to the fact that structure learning becomes unreliable in heavily contaminated graphs. STABLE outperforms ProGNN due to the addition of a large number of reliable edges to the graph.
- Rand, Deg, and Guard apply different strategies for edge pruning based on various node information. Guard builds upon the former two methods by introducing a scoring function based on gradients and node degrees to filter out noisy edges in the graph, which achieves the second-best performance in targeted attack scenarios. GDDM achieves the best performance due to the powerful denoising capabilities of graph diffusion models and specific designed denoising strategy for targeted attack scenarios.
- GDDM outperforms other baseline methods across most perturbation numbers, in both targeted and non-targeted attacks. Moreover, as the perturbation number increases, GDDM experiences a significantly smaller performance decline. This advantage is attributed to the strong recovery capability of the diffusion model in highly disruptive scenarios, along with our tailored denoising strategies and components that leverage structural and feature information for guidance.

5.2.2 Performance Against Non-targeted Attack. The performance under non-targeted attack is shown in Fig. 4. We chose the powerful attack method GraD which is an improved version of Metattack [44] as attacker to perturb graph structure. As we can see, GDDM is

competitive compared to Sota methods, and in most cases, its performance outperforms other baseline methods. Together with the observations from Section 5.2.1, we can conclude that GDDM is capable of effectively defending against both targeted and non-targeted attacks.

5.3 Impact of Tailored Attack-specific Denoising Strategies (RQ2)

To validate the effectiveness of our proposed Tailored Attack-specific Denoising Strategies (TADS) for targeted attacks, we conducted separate experiments in a targeted attack scenario using both GDDM’s denoising strategy designed for targeted attacks and non-targeted attacks. The experimental results are shown in Table 2, where GDDM represents the performance of GDDM using the denoising strategy designed for targeted attacks in a targeted attack scenario, and GDDM w/o TADS represents the performance of GDDM using the denoising strategy for non-targeted attacks in the same targeted attack scenario. The results indicate that the performance of GDDM in the targeted attack scenario significantly improves when using the TADS, demonstrating that GDDM uses TADS to achieve targeted protection by focusing on the attacked nodes.

5.4 Ablation Study (RQ3)

To gain a deeper understanding of how different components impact the model’s performance, we conduct an ablation study to evaluate the contributions of the various components in GDDM:

- **GDDM w/o NFCR:** the proposed GDDM without the Node Feature-Constrained Regularizer.
- **GDDM w/o GSDR:** the proposed GDDM without the Graph Structure-Driven Refiner.

We use the hyper-parameters that achieve the best performance in our main experiment and report the results of 10 runs in Table 3. The results on the chameleon dataset are provided in the Appendix B.3. By comparing the full GDDM model with its ablation versions **GDDM w/o GSDR**, **GDDM w/o NFCR**, we observe that the Graph Structure-Driven Refiner plays a crucial role in GDDM. This component guides the generation process using the structure of the attacked graph, ensuring the basic graph fidelity of the denoised graph. Furthermore, we also observe that both feature smoothness guiding and node degree guiding consist in the Node Feature-Constrained Regularizer future enhance the defense performance. The above two experimental phenomena highlight the importance of graph fidelity in defending against adversarial attacks in graph diffusion models.

5.5 Flexibility Analysis (RQ4)

We analyze the flexibility of GDDM. For the results, please refer to Appendix B.4.

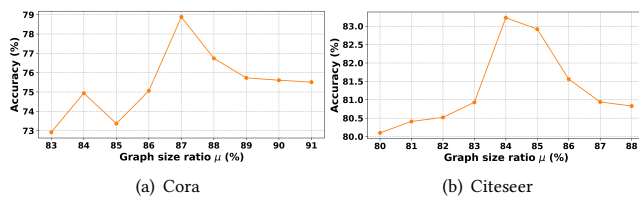
5.6 Parameter Analysis (RQ5)

Drawing from our experimental observations, the graph size ratio μ plays a critical role in optimizing performance. Accordingly, we systematically vary its value to evaluate its influence on the performance of GDDM. As shown in Fig. 5, we conduct experiments using the non-targeted attack method GraD on Cora and Citeseer datasets with a larger perturbation ratio (25%). It is worth noting that as the graph size ratio μ increases, the model’s performance first improves and then declines. This may be because a graph size

Table 3: Ablation experiments under different types of attack methods (GraD and Nettack).

Dataset	Cora					Citeseer				
Ptb Rate	5%	10%	15%	20%	25%	5%	10%	15%	20%	25%
GDDM w/o GSDR	32.49±0.47	32.49±0.47	32.49±0.47	32.49±0.47	32.49±0.47	33.19±0.62	33.19±0.62	33.19±0.62	33.19±0.62	33.19±0.62
GDDM w/o NFCR	77.76±0.45	75.65±0.47	72.51±0.32	69.77±0.50	66.85±0.28	68.75±0.29	66.76±0.52	65.67±0.47	64.01±0.72	60.68±0.38
GDDM	78.72±0.54	77.20±0.34	73.35±0.40	72.00±0.50	69.80±0.32	69.60±0.35	67.71±0.43	66.74±0.40	64.82±0.59	61.49±0.47
Ptb Num	1	2	3	4	5	1	2	3	4	5
GDDM w/o GSDR	42.41±3.01	42.41±3.01	42.41±3.01	42.41±3.01	42.41±3.01	56.90±4.37	56.90±4.37	56.90±4.37	56.90±4.37	56.90±4.37
GDDM w/o NFCR	81.12±1.21	81.01±1.06	80.56±1.01	79.55±1.40	78.09±1.44	81.45±1.30	81.15±1.43	81.25±1.04	82.08±1.38	81.04±1.12
GDDM	81.34±1.43	81.46±1.03	80.78±0.93	79.77±1.01	78.65±1.74	82.50±1.21	81.25±1.47	81.87±1.06	82.60±1.61	81.46±1.02

ratio that is too small can cause the model to remove clean edges from the attacked graph, while a ratio that is too large may lead to insufficient removal of noisy edges. Therefore, we select an optimal graph size ratio to achieve the best model performance.

**Figure 5: Graph size ratio parameter analysis.**

6 Conclusion

Graph Neural Networks (GNNs) are highly sensitive to adversarial attacks on graph structures. To effectively defend against different types of adversarial attacks that can poison GNNs, we propose a novel graph purification method GDDM in this work. This method leverages the powerful denoising capabilities of diffusion models, supplemented by multiple key components and denoising strategies to purify the attacked graphs, thereby effectively reducing the impact of different types of adversarial attacks on GNNs. Our experiments demonstrate that GDDM is highly competitive in both targeted and non-targeted attack scenarios, outperforming SOTA baseline methods in most cases.

References

- [1] Nicolas Carlini, Jamie Hayes, Milad Nasr, Matthew Jagielski, Vikash Swag, Florian Tramer, Borja Balle, Daphne Ippolito, and Eric Wallace. 2023. Extracting training data from diffusion models. In *32nd USENIX Security Symposium (USENIX Security 23)*. 5253–5270.
- [2] Jinyin Chen, Yangyang Wu, Xuanheng Xu, Yixian Chen, Haibin Zheng, and Qi Xuan. 2018. Fast gradient attack on network embedding. *arXiv preprint arXiv:1809.02797* (2018).
- [3] Shoufa Chen, Peize Sun, Yibing Song, and Ping Luo. 2023. Diffusiondet: Diffusion model for object detection. In *Proceedings of the IEEE/CVF international conference on computer vision*. 19830–19843.
- [4] Xiaohui Chen, Jiaxing He, Xu Han, and Li-Ping Liu. 2023. Efficient and degree-guided graph generation via discrete diffusion modeling. *arXiv preprint arXiv:2305.04111* (2023).
- [5] Tyler Derr, Yao Ma, Wenqi Fan, Xiaorui Liu, Charu Aggarwal, and Jiliang Tang. 2020. Epidemic graph convolutional network. In *Proceedings of the 13th International Conference on Web Search and Data Mining*. 160–168.
- [6] Tim Dockhorn, Arash Vahdat, and Karsten Kreis. 2022. Genie: Higher-order denoising diffusion solvers. *Advances in Neural Information Processing Systems* 35 (2022), 30150–30166.
- [7] Negin Entezari, Saba A Al-Sayouri, Amirali Darvishzadeh, and Evangelos E Papalexakis. 2020. All you need is low (rank) defending against adversarial attacks on graphs. In *Proceedings of the 13th international conference on web search and data mining*. 169–177.
- [8] Wenqi Fan, Xiaorui Liu, Wei Jin, Xiangyu Zhao, Jiliang Tang, and Qing Li. 2022. Graph trend filtering networks for recommendation. In *Proceedings of the 45th international ACM SIGIR conference on research and development in information retrieval*. 112–121.
- [9] Wenqi Fan, Yao Ma, Qing Li, Yuan He, Eric Zhao, Jiliang Tang, and Dawei Yin. 2019. Graph neural networks for social recommendation. In *The world wide web conference*. 417–426.
- [10] Sicheng Gao, Xuhui Liu, Bohan Zeng, Sheng Xu, Yanjing Li, Xiaoyan Luo, Jianzhuang Liu, Xiantong Zhen, and Baochang Zhang. 2023. Implicit diffusion models for continuous super-resolution. In *Proceedings of the IEEE/CVF conference on computer vision and pattern recognition*. 10021–10030.
- [11] Simon Geisler, Tobias Schmidt, Hakan Şirin, Daniel Zügner, Aleksandar Bojchevski, and Stephan Günnemann. 2021. Robustness of graph neural networks at scale. *Advances in Neural Information Processing Systems* 34 (2021), 7637–7649.
- [12] Will Hamilton, Zhitao Ying, and Jure Leskovec. 2017. Inductive representation learning on large graphs. *Advances in neural information processing systems* 30 (2017).
- [13] John Hammersley. 2013. *Monte carlo methods*. Springer Science & Business Media.
- [14] Xiangnan He, Kuan Deng, Xiang Wang, Yan Li, Yongdong Zhang, and Meng Wang. 2020. Lightgcn: Simplifying and powering graph convolution network for recommendation. In *Proceedings of the 43rd International ACM SIGIR conference on research and development in Information Retrieval*. 639–648.
- [15] Jonathan Ho, Ajay Jain, and Pieter Abbeel. 2020. Denoising diffusion probabilistic models. *Advances in neural information processing systems* 33 (2020), 6840–6851.
- [16] Eric Jang, Shixiang Gu, and Ben Poole. 2016. Categorical reparameterization with gumbel-softmax. *arXiv preprint arXiv:1611.01144* (2016).
- [17] Wei Jin, Tyler Derr, Yiqi Wang, Yao Ma, Zitao Liu, and Jiliang Tang. 2021. Node similarity preserving graph convolutional networks. In *Proceedings of the 14th ACM international conference on web search and data mining*. 148–156.
- [18] Wei Jin, Yaxing Li, Han Xu, Yiqi Wang, Shuiwang Ji, Charu Aggarwal, and Jiliang Tang. 2021. Adversarial attacks and defenses on graphs. *ACM SIGKDD Explorations Newsletter* 22, 2 (2021), 19–34.
- [19] Wei Jin, Yao Ma, Xiaorui Liu, Xianfeng Tang, Suhang Wang, and Jiliang Tang. 2020. Graph structure learning for robust graph neural networks. In *Proceedings of the 26th ACM SIGKDD international conference on knowledge discovery & data mining*. 66–74.
- [20] Wei Jin, Tong Zhao, Jiayuan Ding, Yozen Liu, Jiliang Tang, and Neil Shah. 2023. Empowering Graph Representation Learning with Test-Time Graph Transformation. In *The Eleventh International Conference on Learning Representations*. <https://openreview.net/forum?id=Lnx15pr018>
- [21] Jaehyeon Jo, Seul Lee, and Sung Ju Hwang. 2022. Score-based generative modeling of graphs via the system of stochastic differential equations. In *International conference on machine learning*. PMLR, 10362–10383.
- [22] Thomas N Kipf and Max Welling. 2016. Semi-supervised classification with graph convolutional networks. *arXiv preprint arXiv:1609.02907* (2016).
- [23] Thomas N. Kipf and Max Welling. 2017. Semi-Supervised Classification with Graph Convolutional Networks. In *International Conference on Learning Representations (ICLR)*.
- [24] Jintang Li, Jie Liao, Ruofan Wu, Liang Chen, Zibin Zheng, Jiawang Dan, Changhua Meng, and Weiqiang Wang. 2023. GUARD: Graph universal adversarial defense. In *Proceedings of the 32nd ACM International Conference on Information and Knowledge Management*. 1198–1207.
- [25] Kuan Li, Yang Liu, Xiang Ao, Jianfeng Chi, Jinghua Feng, Hao Yang, and Qing He. 2022. Reliable representations make a stronger defender: Unsupervised structure refinement for robust gnn. In *Proceedings of the 28th ACM SIGKDD conference on knowledge discovery and data mining*. 925–935.
- [26] Gang Liu, Eric Inae, Tong Zhao, Jiaxin Xu, Tengfei Luo, and Meng Jiang. 2024. Data-centric learning from unlabeled graphs with diffusion model. *Advances in neural information processing systems* 36 (2024).
- [27] Xiaorui Liu, Wei Jin, Yao Ma, Yaxin Li, Hua Liu, Yiqi Wang, Ming Yan, and Jiliang Tang. 2021. Elastic graph neural networks. In *International Conference on Machine Learning*. PMLR, 6837–6849.
- [28] Zihan Liu, Yun Luo, Lirong Wu, Zicheng Liu, and Stan Z Li. 2023. Towards reasonable budget allocation in untargeted graph structure attacks via gradient debias. *arXiv preprint arXiv:2304.00010* (2023).
- [29] Felix Mujkanovic, Simon Geisler, Stephan Günnemann, and Aleksandar Bojchevski. 2022. Are defenses for graph neural networks robust? *Advances in Neural Information Processing Systems* 35 (2022), 8954–8968.
- [30] Weili Nie, Brandon Guo, Yujia Huang, Chaowei Xiao, Arash Vahdat, and Anima Anandkumar. 2022. Diffusion models for adversarial purification. *arXiv preprint arXiv:2205.07460* (2022).
- [31] William Peebles and Saining Xie. 2023. Scalable diffusion models with transformers. In *Proceedings of the IEEE/CVF International Conference on Computer Vision*. 4195–4205.
- [32] Jascha Sohl-Dickstein, Eric Weiss, Niru Maheswaranathan, and Surya Ganguli. 2015. Deep unsupervised learning using nonequilibrium thermodynamics. In *International conference on machine learning*. PMLR, 2256–2265.
- [33] Lichao Sun, Yingdong Dou, Carl Yang, Kai Zhang, Ji Wang, S Yu Philip, Lifang He, and Bo Li. 2022. Adversarial attack and defense on graph data: A survey. *IEEE Transactions on Knowledge and Data Engineering* 35, 8 (2022), 7693–7711.
- [34] Zhiqing Sun and Yiming Yang. 2023. Difusco: Graph-based diffusion solvers for combinatorial optimization. *Advances in Neural Information Processing Systems* 36 (2023), 3706–3731.
- [35] Petar Veličković, Guillem Cucurull, Arantxa Casanova, Adriana Romero, Pietro Lio, and Yoshua Bengio. 2018. Graph attention networks. (2018).
- [36] Clement Vignac, Igor Krawczuk, Antoine Siraudin, Bohan Wang, Volkan Cevher, and Pascal Frossard. 2022. Digress: Discrete denoising diffusion for graph generation. *arXiv preprint arXiv:2209.14734* (2022).
- [37] Huijun Wu, Chen Wang, Yuriy Tyshetskiy, Andrew Docherty, Kai Lu, and Liming Zhu. 2019. Adversarial examples on graph data: Deep insights into attack and defense. *arXiv preprint arXiv:1903.01610* (2019).
- [38] Mingyang Wu, Xiaohui Chen, and Liping Liu. 2023. EDGE++: Improved Training and Sampling of EDGE. *arXiv preprint arXiv:2310.14441* (2023).
- [39] Bin Xia, Yulun Zhang, Shiyin Wang, Yitong Wang, Xinglong Wu, Yapeng Tian, Wenming Yang, and Luc Van Gool. 2023. Diffir: Efficient diffusion model for image restoration. In *Proceedings of the IEEE/CVF International Conference on Computer Vision*. 13095–13105.
- [40] Donghan Yu, Ruohong Zhang, Zhengbao Jiang, Yuexin Wu, and Yiming Yang. 2021. Graph-revised convolutional network. In *Machine Learning and Knowledge Discovery in Databases: European Conference, ECML PKDD 2020, Ghent, Belgium, September 14–18, 2020, Proceedings, Part III*. Springer, 378–393.
- [41] Xiang Zhang and Marinka Zitnik. 2020. Gnn-guard: Defending graph neural networks against adversarial attacks. *Advances in neural information processing systems* 33 (2020), 9263–9275.
- [42] Dingyuan Zhu, Ziwei Zhang, Peng Cui, and Wenwu Zhu. 2019. Robust graph convolutional networks against adversarial attacks. In *Proceedings of the 25th ACM SIGKDD international conference on knowledge discovery & data mining*. 1399–1407.
- [43] Daniel Zügner, Amir Akbarnejad, and Stephan Günnemann. 2018. Adversarial attacks on neural networks for graph data. In *Proceedings of the 24th ACM SIGKDD international conference on knowledge discovery & data mining*. 2847–2856.
- [44] Daniel Zügner and Stephan Günnemann. 2019. Adversarial Attacks on Graph Neural Networks via Meta Learning. In *International Conference on Learning Representations (ICLR)*.

A Detailed Implementations

A.1 Derivation Process of the Posterior

$$\begin{aligned}
 q(\mathbf{A}^{t-1}|\mathbf{A}^t, \mathbf{s}^t, \mathbf{A}^0) &= \frac{q(\mathbf{A}^{t-1}, \mathbf{A}^t, \mathbf{s}^t|\mathbf{A}^0)}{q(\mathbf{A}^t, \mathbf{s}^t|\mathbf{A}^0)} \\
 &= \frac{q(\mathbf{A}^t|\mathbf{A}^{t-1}, \mathbf{A}^0)q(\mathbf{s}^t|\mathbf{A}^0, \mathbf{A}^t, \mathbf{A}^{t-1})q(\mathbf{A}^{t-1}|\mathbf{A}^0)}{q(\mathbf{A}^t, \mathbf{s}^t|\mathbf{A}^0)} \\
 &= \frac{q(\mathbf{A}^t|\mathbf{A}^{t-1})q(\mathbf{s}^t|\mathbf{A}^t, \mathbf{A}^{t-1})q(\mathbf{A}^{t-1}|\mathbf{A}^0)}{q(\mathbf{A}^t|\mathbf{A}^0)q(\mathbf{s}^t|\mathbf{A}^t, \mathbf{A}^0)}.
 \end{aligned} \tag{20}$$

A.2 Information Propagation Process Module

In the information propagation process, the node representation \mathbf{Z} and the representation \mathbf{t}_{emb} of the timestep t are concatenated as the input of GT. GRU adaptively retains important information inputting the output of GT and the nodes' hidden features \mathbf{H} :

$$\mathbf{Z}^l = \text{concat}(\mathbf{Z}^l \parallel \mathbf{t}_{emb} \mathbf{1}^T), \tag{21}$$

$$\mathbf{Z}^l = \text{GT}(\mathbf{Z}^l, \mathbf{A}^t), \tag{22}$$

$$\mathbf{Z}^l, \mathbf{H}^{l+1} = \text{GRU}(\mathbf{Z}^l, \mathbf{H}^l), \tag{23}$$

where \mathbf{t}_{emb} is the representation of timestep t . \mathbf{A}^t is the adjacency matrix of the graph at the current timestep t . $\text{GT}(\cdot)$ represents Graph Transformer, which performs attentive information propagation between nodes, allowing each node to aggregate local feature information from its neighborhood in the graph. $\text{GRU}(\cdot)$ represents Gated Recurrent Unit (GRU).

To update the global contextual feature \mathbf{c}^l , the representation of each node and the current global contextual feature \mathbf{c}^l are concatenated and applied a mean operation as the input of a MLP. The output of the MLP serves as the global contextual feature for the next layer:

$$\mathbf{c}^{l+1} = \text{MLP}(\text{mean}(\text{concat}(\mathbf{Z}^l \parallel \mathbf{c}^l \mathbf{1}^T))). \tag{24}$$

Finally, the node representations \mathbf{Z} and the global contextual feature \mathbf{c}^{l+1} are summed to obtain the initial node representations for the next MPM:

$$\mathbf{Z}^{l+1} = \mathbf{Z}^l + \mathbf{c}^{l+1} \mathbf{1}^T. \tag{25}$$

A.3 Algorithm of Training Phase

The training phase of GDDM is shown in Algorithm 2.

Algorithm 2 The Training Phase of GDDM

Input: The clean graph adjacency matrix \mathbf{A}^0 , diffusion schedule β , the learnable parameter θ .

- 1: **while** model convergence **do**
 - 2: Sample $t \sim \mathcal{U}[1, T]$, and obtain $t - 1$.
 - 3: Draw $\mathbf{A}^{t-1} \sim q(\mathbf{A}^{t-1}|\mathbf{A}^0)$ and $\mathbf{A}^t \sim q(\mathbf{A}^t|\mathbf{A}^{t-1})$.
 - 4: Obtain \mathbf{s}^t with \mathbf{A}^{t-1} and \mathbf{A}^t .
 - 5: Optimize the parameter θ by minimizing $\log \frac{p_\theta(\mathbf{A}^{t-1}|\mathbf{A}^t, \mathbf{s}^t)}{q(\mathbf{A}^{t-1}|\mathbf{A}^t, \mathbf{A}^0, \mathbf{s}^t)}$.
 - 6: **end while**
-

A.4 The Inference Phase of GDDM for Targeted Attack

The detail of the Tailored Attack-specific Denoising Strategies (TADS) is shown in Figure 6.

B Experiments Detail

B.1 Dataset

The statistics are listed in Tabel 4. Cora and Citeseer are citation networks where nodes represent papers from seven and six research categories, respectively, and edges denote citation links. Chameleon is a Wikipedia graph with edges representing mutual links and nodes often connect to different classes.

Table 4: Statistics of the experimental data.

Dataset	N	E	Classes	Features
Cora	2,708	5,278	7	1,433
Citeseer	3,327	4,552	6	3,703
Chameleon	2,277	31,371	5	2,325

B.2 Baselines

- **GCN:** GCN is a widely used graph convolutional network grounded in spectral graph theory. It applies convolution operations on graphs to capture the relationships between nodes based on their connectivity.
- **Jaccard:** Jaccard prunes edges based on the feature similarity between nodes, as adversarial attacks tend to connect dissimilar nodes in the graph.
- **SVD:** SVD removes the high-rank perturbations introduced by adversarial attacks by the low-rank approximation of the attacked graph, enhancing the robustness of GNN model.
- **ProGNN:** ProGNN mitigates the negative impact of adversarial attacks on GNN models by optimizing the adjacency matrix of the attacked graph using regularization terms based on feature smoothness, low-rank, and sparsity.
- **Guard:** Guard uses a scoring function based on node degree and gradient to identify anchor nodes (attacker nodes), then removes all edges between the anchor nodes and the target node to ensure the target node is protected from attacks.
- **Rand:** Rand is a baseline version of Guard, where the strategy for selecting anchor nodes is replaced by random selection instead of using a scoring function.
- **Deg:** Deg is another baseline version of Guard, where the strategy for selecting anchor nodes is based on node degree, as lower-degree nodes are more likely to become anchor nodes.
- **STABLE:** STABLE is an unsupervised method for optimizing graph structure, which leverages a specially designed robust GCN to effectively defend against adversarial attacks on graph data.
- **Grad:** Grad introduces an improved attack objective function that enables the attack model to target medium-confidence nodes, thereby increasing attack efficiency.

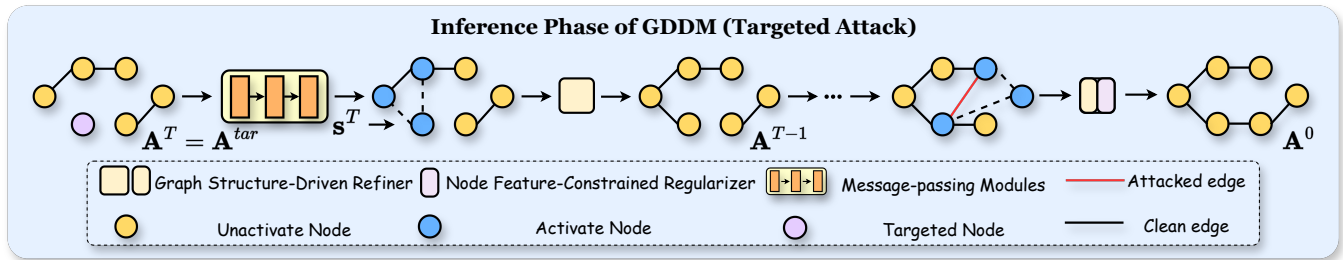


Figure 6: The Inference Phase of GDDM for Targeted Attacks.

- **Nettack:** Nettack is a greedy-based attack method that perturbs targeted nodes in a graph while preserving the node degree distribution and feature co-occurrence.

B.3 Ablation Study in Chameleon Dataset

The ablation study results of our proposed method on the Chameleon dataset are shown in Table 5. Due to the inherent heterogeneity of the Chameleon dataset, the introduction of feature smoothness sometimes does not lead to performance improvement. Therefore, additional auxiliary information may be required to further enhance GDDM’s denoising capabilities for heterogeneous graphs.

B.4 Flexibility

To assess the flexibility of GDDM, specifically its plug-and-play capability, we conducted experiments across various GNN classifiers. The results are presented in Table 6 and Table 7. We observed that GDDM demonstrates a highly significant denoising capability on the attacked graphs across three different GNN classifiers. This indicates that GDDM can be flexibly integrated between upstream attack methods and downstream GNN classifiers, significantly enhancing the robustness of the GNN classifiers.

Received 20 February 2007; revised 12 March 2009; accepted 5 June 2009

Table 5: Ablation experiments under different types of attack methods (GraD and Nettack).

Dataset	Chameleon					
	Ptb Rate	5%	10%	15%	20%	25%
GDDM w/o GSDR		23.69±0.53	23.69±0.53	23.69±0.53	23.69±0.53	23.69±0.53
GDDM w/o NFCR		49.09±0.53	46.71±1.01	45.88±0.71	47.46±1.53	44.89±0.56
GDDM		49.46±0.72	48.35±0.62	46.89±0.84	46.56±0.61	45.08±0.64
Ptb Num		1	2	3	4	5
GDDM w/o GSDR		30.65±3.00	30.65±3.00	30.65±3.00	30.65±3.00	30.65±3.00
GDDM w/o NFCR		56.56±1.02	55.82±0.52	55.54±0.59	55.00±0.63	53.23±0.76
GDDM		58.45±0.90	56.60±0.69	55.48±0.97	54.83±0.48	54.76±0.81

Table 6: Node classification performance for different backbone under targeted attack (Nettack).

Datasets	Ptb Num	GCN	with GDDM	GraphSage	with GDDM	GAT	with GDDM
Cora	0	81.46±1.04	82.02±1.00	80.86±2.10	81.55±1.10	84.48±1.88	83.97±1.90
	1	75.51±1.31	81.34±1.43	75.52±1.69	81.21±2.24	79.48±3.13	81.03±2.18
	2	71.01±1.57	81.46±1.03	70.69±1.72	80.34±1.92	73.97±1.96	83.10±2.15
	3	67.87±1.76	80.78±0.93	66.37±2.91	81.55±2.05	66.38±5.19	80.00±1.38
	4	63.93±1.98	79.77±1.01	63.45±2.41	81.37±2.01	60.17±5.26	77.24±2.15
	5	57.64±1.88	78.65±1.74	57.93±2.34	78.97±1.69	52.41±4.44	76.21±1.50
	Mean	69.72	80.56	69.13	80.83	69.48	80.26
Citeseer	0	83.12±1.12	83.03±1.05	80.99±2.11	80.42±2.22	82.96±1.17	83.24±1.60
	1	76.25±1.38	82.50±1.21	74.22±1.10	79.72±2.01	75.92±6.62	82.25±2.20
	2	60.10±4.52	81.25±1.47	61.26±0.46	79.72±2.54	50.99±4.99	82.95±2.31
	3	54.48±1.92	81.87±1.06	51.27±7.11	81.27±1.55	47.46±5.74	81.83±2.39
	4	48.44±2.43	82.60±1.61	41.83±5.81	79.72±1.91	38.73±5.54	82.25±1.91
	5	43.33±2.95	81.46±1.02	35.63±4.92	80.28±1.99	34.93±4.26	80.56±2.58
	Mean	60.95	82.00	57.53	80.19	55.17	82.18
Chameleon	0	59.20±0.42	58.01±0.86	42.37±2.55	42.16±2.11	49.17±2.36	49.10±2.67
	1	54.58±0.70	58.45±0.90	37.41±2.41	40.14±1.96	42.37±3.46	50.76±1.44
	2	50.62±0.87	56.60±0.69	32.37±2.02	40.50±1.67	36.47±2.86	47.98±1.88
	3	47.20±0.67	55.48±0.97	30.21±2.37	38.17±2.60	28.20±3.34	47.05±1.90
	4	42.84±1.48	54.83±0.48	27.23±2.57	37.95±2.75	26.69±4.64	48.42±1.64
	5	40.63±2.19	54.76±0.81	25.54±3.31	37.84±1.90	23.96±3.71	46.43±1.64
	Mean	49.18	56.34	32.51	39.46	34.48	48.29

Table 7: Node classification performance for different backbone under non-targeted attack (GraD).

Datasets	Ptb Num	GCN	with GDDM	GraphSage	with GDDM	GAT	with GDDM
Cora	0%	82.38±0.60	81.38±0.51	81.22±0.72	80.11±0.53	83.28±0.35	82.02±0.62
	5%	76.81±0.85	78.72±0.54	72.10±1.36	77.30±0.44	80.23±0.79	80.61±0.85
	10%	69.84±1.19	77.20±0.34	66.69±3.22	75.14±0.41	75.38±0.77	78.68±0.99
	15%	62.39±2.16	73.35±0.40	62.86±2.38	72.10±0.55	69.37±1.17	76.80±0.58
	20%	55.34±2.11	72.00±0.50	58.32±2.13	70.47±0.43	63.74±2.04	75.02±0.90
	25%	49.73±2.33	69.80±0.32	54.10±1.81	69.22±0.88	58.24±2.02	74.49±0.90
	Mean	66.24	75.41	65.88	74.06	71.71	77.94
Citeseer	0%	69.83±0.23	69.50±0.33	69.76±0.51	69.58±0.57	70.77±0.91	69.62±1.10
	5%	62.83±1.34	69.60±0.35	60.12±1.32	68.62±0.95	68.40±0.75	69.50±1.43
	10%	57.29±1.19	67.71±0.43	55.94±2.62	67.09±0.97	63.48±0.88	68.62±0.80
	15%	53.32±1.28	66.74±0.40	52.93±2.32	65.22±0.76	58.60±1.68	66.77±1.11
	20%	47.68±1.25	64.82±0.59	49.57±2.57	63.56±0.84	55.26±0.97	65.43±0.69
	25%	43.90±1.23	61.49±0.47	47.52±3.30	61.18±1.12	51.59±0.81	63.32±0.82
	Mean	55.81	66.54	55.97	65.88	61.35	67.21
Chameleon	0%	55.64±0.69	54.16±0.51	48.69±1.61	47.72±1.69	56.66±1.17	56.26±1.04
	5%	38.30±1.44	49.46±0.72	41.16±1.51	44.60±1.34	46.88±1.50	52.05±1.18
	10%	32.38±2.37	48.35±0.62	39.76±1.69	44.59±1.55	40.55±3.29	50.34±0.99
	15%	30.09±1.77	46.89±0.84	39.23±1.74	42.74±1.72	37.67±2.33	46.93±0.96
	20%	29.74±2.08	46.56±0.61	38.52±1.87	44.25±1.53	36.55±1.84	47.28±1.45
	25%	28.69±1.55	45.08±0.64	38.06±1.67	42.65±0.99	34.52±2.55	46.71±0.86
	Mean	35.81	48.42	40.90	44.43	42.14	49.93